



# Improving the State Selectivity of Field Ionization with Quantum Control

Vincent C. Gregoric<sup>1</sup>, Ankitha Kannad<sup>1</sup>, Zhimin Cheryl Liu<sup>1</sup>, Thomas J. Carroll<sup>2</sup>, and Michael W. Noel<sup>1</sup>

<sup>1</sup>Department of Physics, Bryn Mawr College, Bryn Mawr, PA 19010 <sup>2</sup>Department of Physics and Astronomy, Ursinus College, Collegeville, PA 19426  
This work was supported by the National Science Foundation under Grants No. 1607335 and No. 1607377 and the Howard Hughes Medical Institute.

## Abstract

The state distribution of a collection of Rydberg atoms can be determined by ionizing the atoms with a slowly increasing electric field, a process known as selective field ionization. Generally, atoms in higher energy states are ionized at lower fields, so ionized electrons which are detected earlier in time can be correlated with higher energy Rydberg states. However, the resolution of this technique is limited by the Stark effect. As the electric field is increased, the electron encounters many avoided Stark level crossings which split the amplitude among many states, thus broadening the time-resolved ionization signal. Previously, we have demonstrated *directed field ionization*, a modification of selective field ionization in which we use a genetic algorithm (GA) to exert quantum control over the time-resolved ionization signal shape of a single Rydberg state. Here, we present an extension of this work to separate the signals from two states which are originally overlapped in our selective field ionization signal.

## Selective Field Ionization

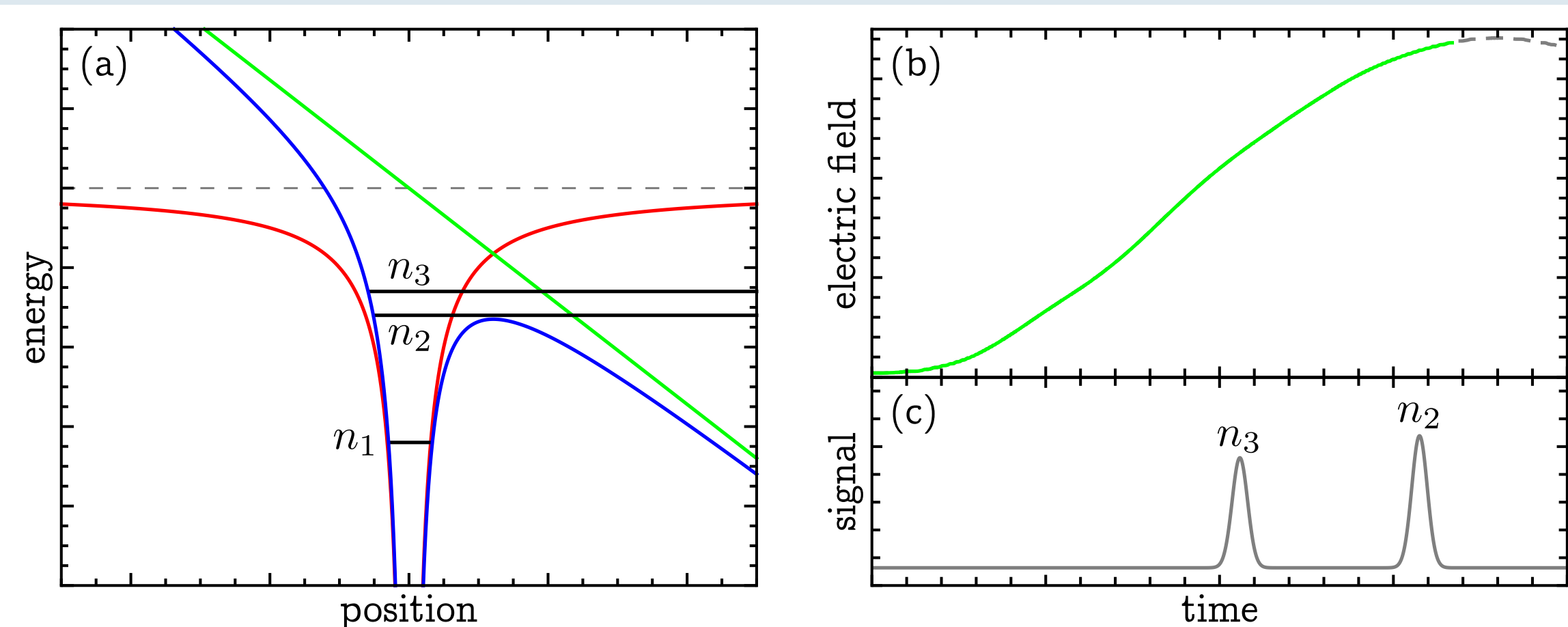


**Figure 1:** Classical description of selective field ionization. (a) The potential for an external electric field (green) is added to the initial Coulombic potential (red). For the total potential (blue), states  $n_2$  and  $n_3$  are no longer bound. (b) The electric field is increased roughly linearly in time, resulting in a time-dependent ionization signal, shown in (c). Different states ionize at different times, providing a state-sensitive detection method.

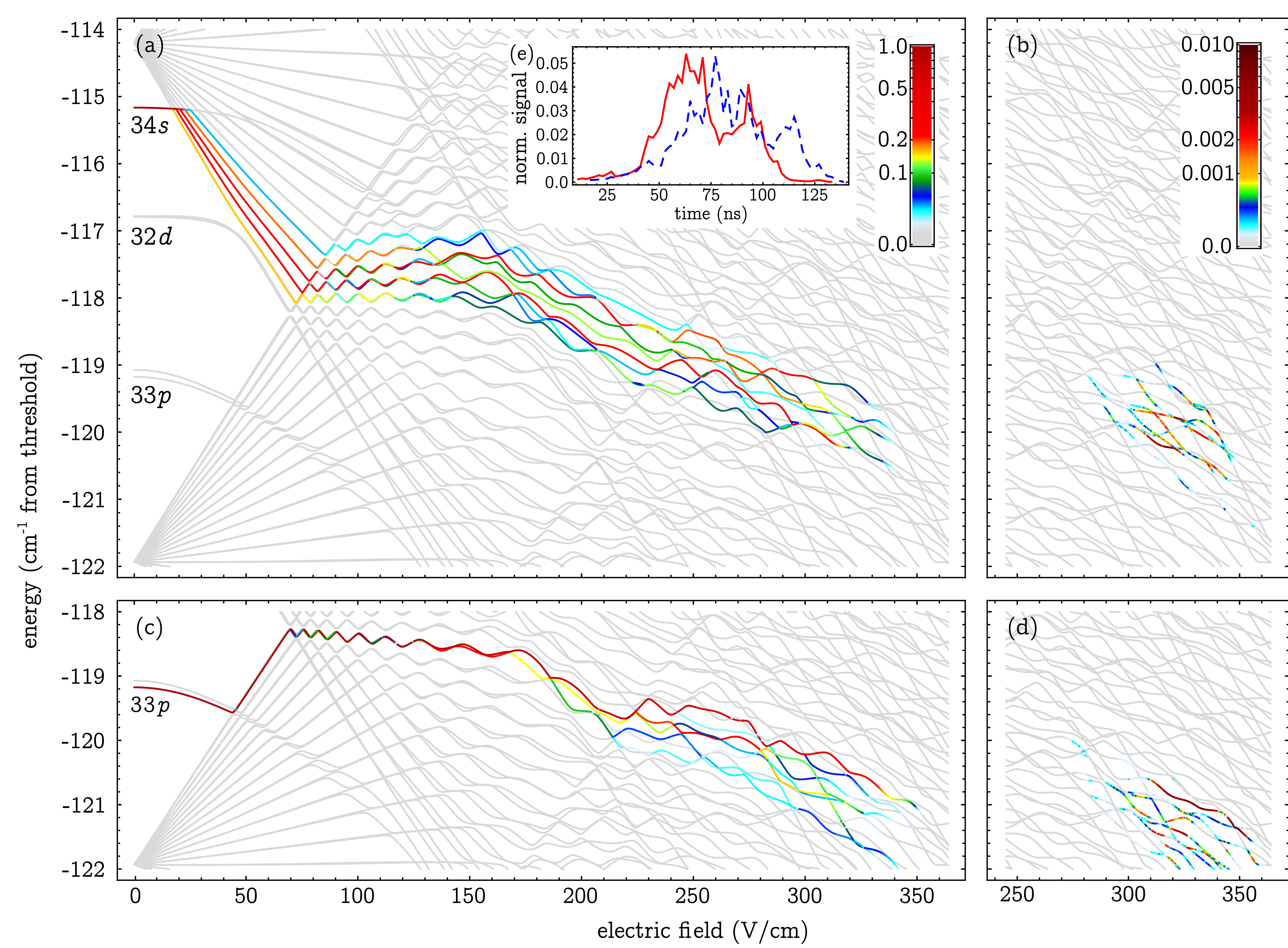


**Figure 2:** Calculated model of selective field ionization. The calculation was performed by constructing the time evolution operator with a basis including the states from  $n = 26$  to  $n = 36$  and at a time resolution of 0.01 ns. The path to ionization for the  $34s$  and  $33p$  initial states are shown in (a) and (c), respectively. Each line is colored according to the population remaining in that state using the legend in (a). The population ionized from each state in each 50 ns time interval for the initially populated  $34s$  and  $33p$  states is shown in (b) and (d) respectively, with each line colored by the legend in (b). Even though the  $34s$  and  $33p$  are ionized from a different, and nearly non-overlapping, set of states, they ionize at roughly the same fields. This is seen clearly in the calculated time-resolved field ionization signal shown in (e), where the  $34s$  (solid, red) and  $33p$  (dashed, blue) signals overlap significantly.

## Experimental Design: Genetic Algorithm

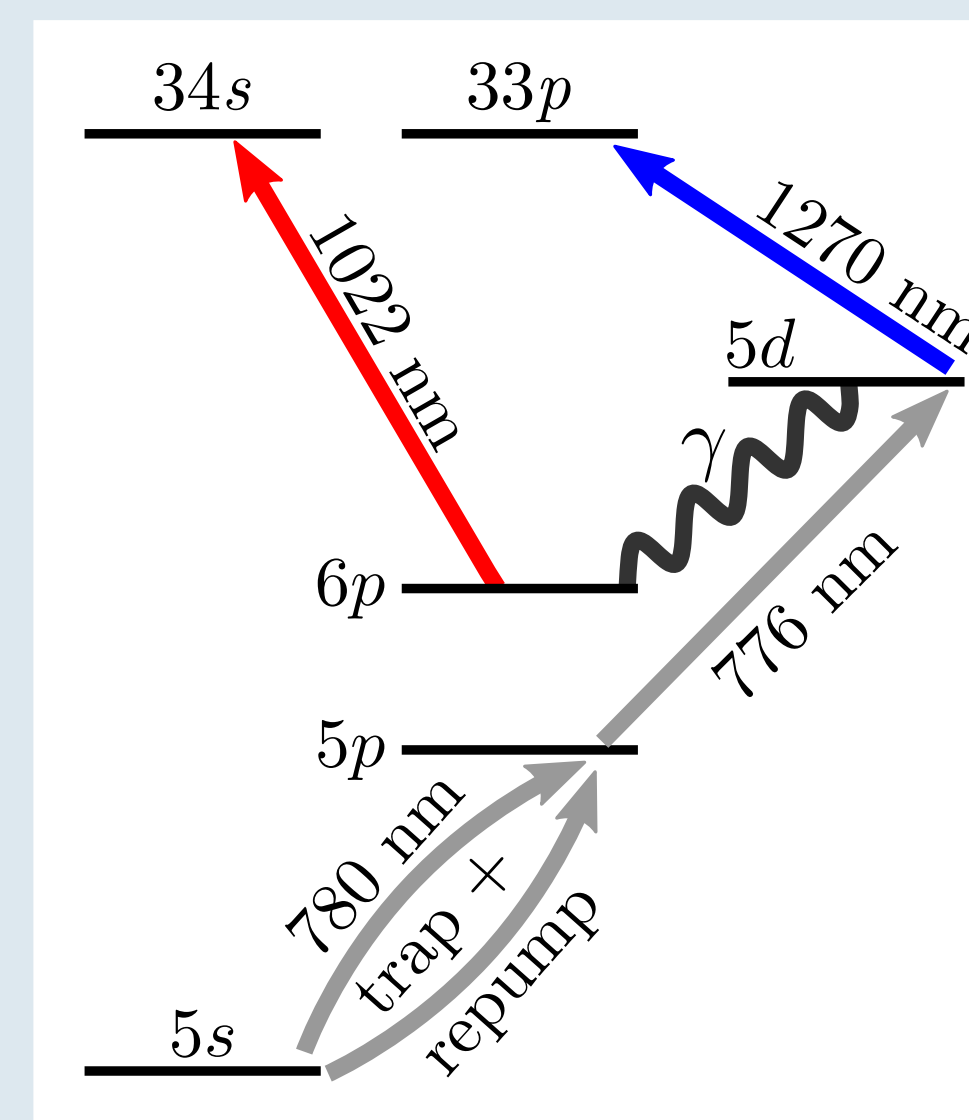


**Figure 3:** Excitation pathway. The  $34s$  and  $33p$  states are excited in multiple steps, driven by lasers at appropriate wavelengths. During the GA, the excitation alternates between the  $34s$  and  $33p$  states by tuning the acoustic frequency of AOMs controlling the 1022 nm and 1270 nm lasers.

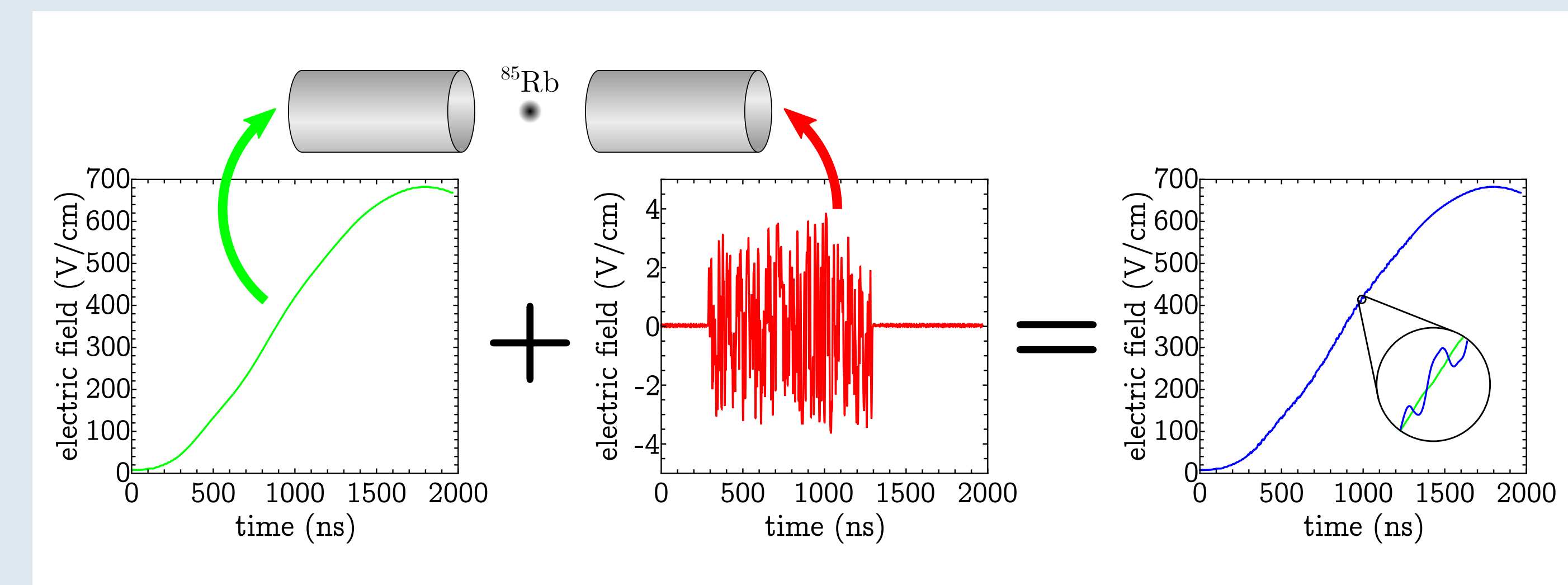


**Figure 4:** Electric fields used in the experiment. The ionizing electric field (green) has an average slow rate of 0.4 (V/cm)/ns, and is applied to a cylinder on one side of our MOT of  $^{85}\text{Rb}$  atoms. An arbitrary waveform generator applies a perturbation (red) to the cylinder on the opposite side of the trap. This perturbation can switch between  $\pm 3.8$  V/cm in 3.3 ns. The total field (blue) experienced by the atoms is the sum of the ionizing field and the perturbing field. While the total field generally increases linearly towards the ionization threshold, the perturbations allow for instantaneous slew rates between  $-1.6$  and  $3.0$  (V/cm)/ns.

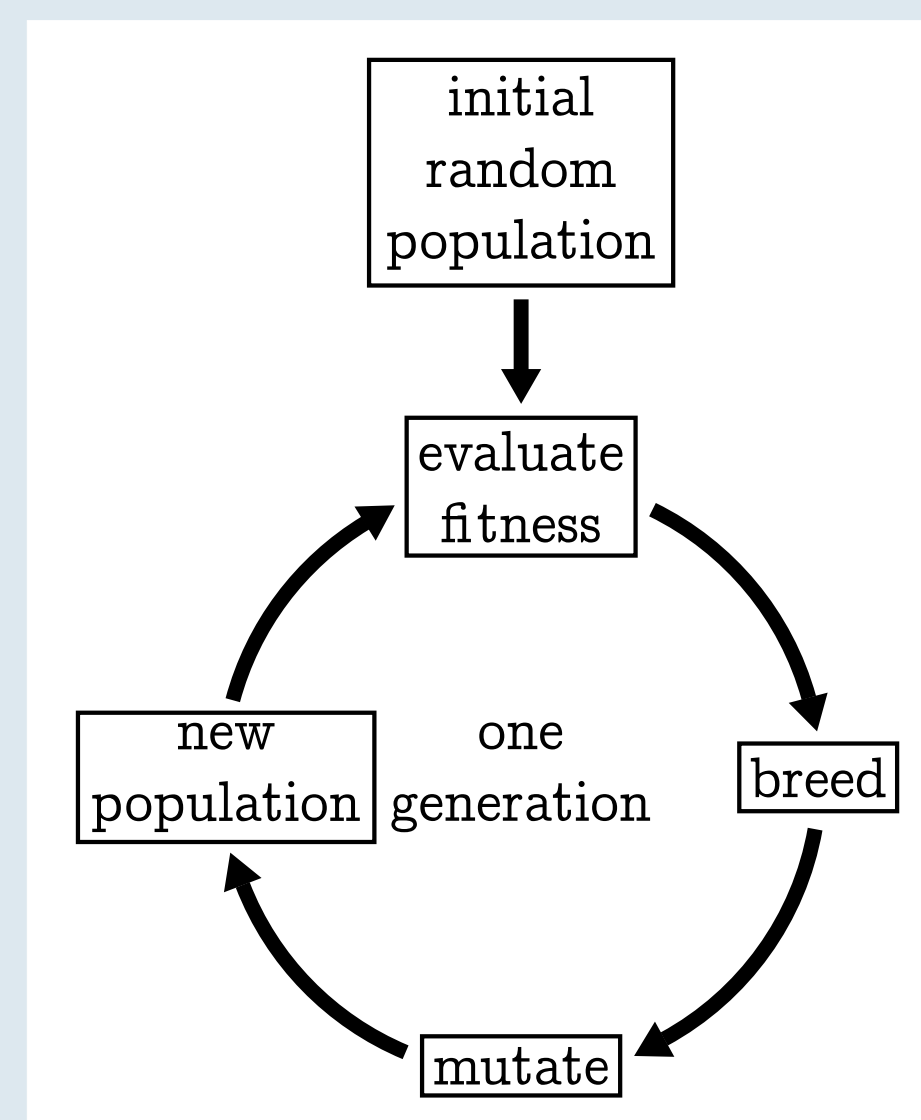


**Figure 5:** Flowchart of the GA used to optimize the perturbations to the ionizing electric field. Beginning with a randomly generated population of perturbations, the algorithm calculates a fitness score for each perturbation which quantifies its ability to manipulate the ionization signal in a desired way. A new generation of perturbations is then created by breeding the successful members of the current generation, and the cycle is repeated.

## Results: Separating the $34s$ and $33p$ States

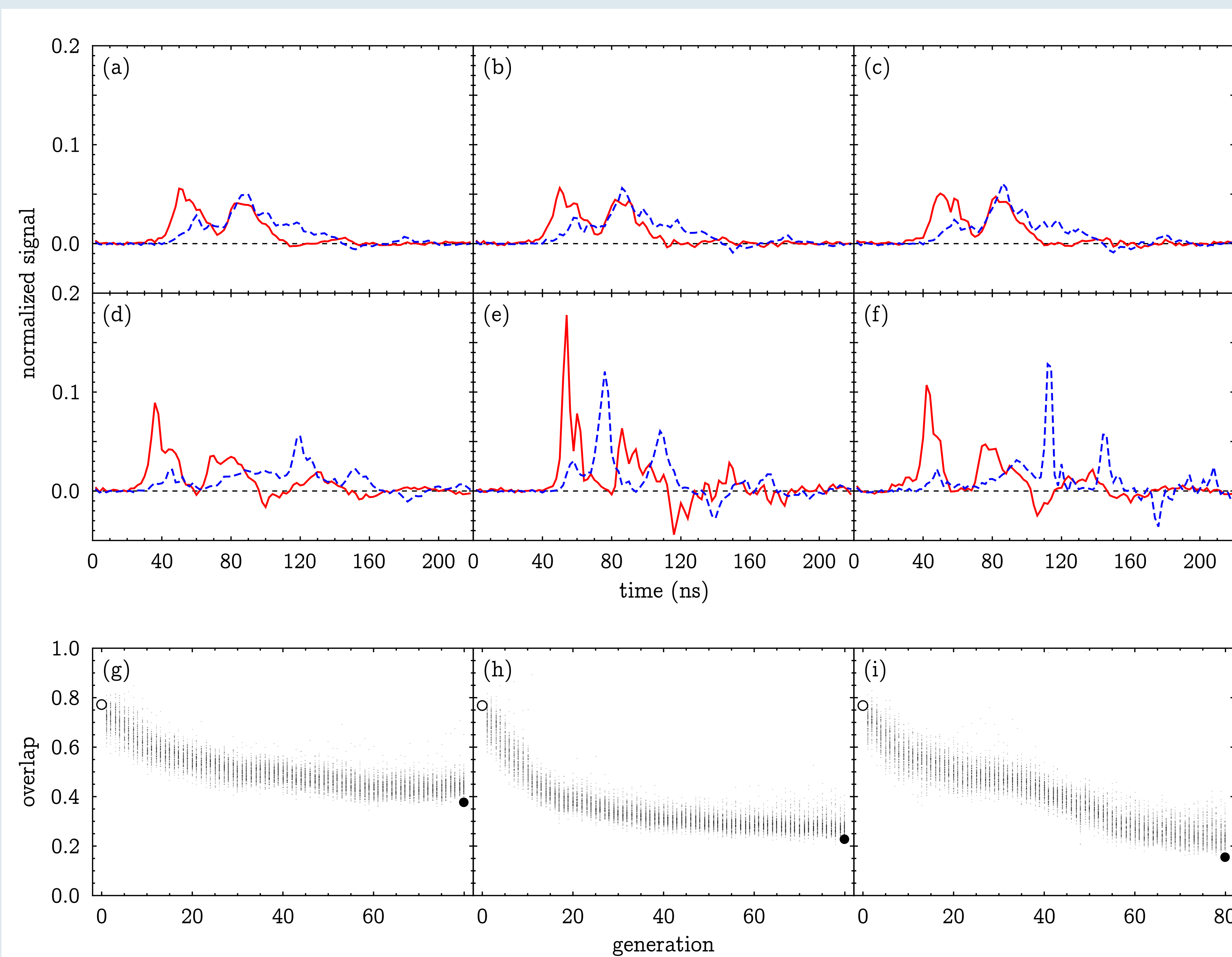


**Figure 6:** GA scans to separate the  $34s$  (red, solid) and  $33p$  (blue, dashed) states. The unperturbed traces are shown in (a)–(c), while the best results from the last generation are shown in (d)–(f). In (g)–(i), the overlap between the two states is plotted vs. generation for each member of the GA population; the large open and filled circles represent the unperturbed overlap and the best overlap in the last generation, respectively. For the left column, a "weighted shift" fitness score was used; the  $33p$  signal was multiplied by a linear weighting function of positive slope, while the  $34s$  signal was multiplied by a negatively-sloped linear weight. This causes the  $p$  state to shift right and the  $s$  state to shift left as the generations progress. The fitness score used in the center column was  $1 - \text{the normalized overlap integral between the } s \text{ and } p \text{ states}$ ; perturbations that minimize the overlap are preferred by the GA. For the right column, a weighted shift fitness score was used for 40 generations before switching to a minimize overlap fitness score. From left to right, the GA was able to decrease the overlap to 38%, 23%, and 15%, respectively (compared to 77% in the unperturbed case).